Functional activity and morphology of isolated rat cardiac mitochondria under calcium overload. Effect of naringin

T. A. Kavalenia
Yanka Kupala State University of Grodno
E. A. Lapshina
Yanka Kupala State University of Grodno
T. V. Ilyich
Yanka Kupala State University of Grodno
Hu-Cheng Zhao
Tsinghua University
I. B. Zavodnik (zavodnik_ib@grsu.by)
Yanka Kupala State University of Grodno

Research Article

Keywords: cardiac mitochondria, calcium ions, ultrastructure, respiratory activity, permeability, flavonoid naringin

Posted Date: July 5th, 2023

DOI: https://doi.org/10.21203/rs.3.rs-3120840/v1

Abstract

The role of calcium-dependent processes in cardiac physiology and pathophysiology as well as the function of mitochondria as a regulator of myocyte calcium homeostasis have been extensively discussed. The aim of the present work was to evaluate the mechanism(s) of modulation of respiratory activity, morphology, permeability transition, and membrane potential of rat cardiac mitochondria by exogenous Ca^{2+} ions in the absence or in the presence of the plant flavonoid glucoside naringin. Low free Ca^{2+} concentrations (40–250 nM) effectively inhibited the respiratory activity of rat heart mitochondria: decreased the rates of succinate-dependent V2 and ADP-stimulated V3 respiration, remaining unaffected the efficacy of oxygen consumption. In the presence of high exogenous Ca^{2+} ion concentrations (the free Ca^{2+} concentration was 550 μM), we observed a dramatic increase in mitochondrial heterogeneity in size and electron density that was connected with calcium-induced opening of the mitochondrial permeability transition pores (MPTP) and membrane depolarization, observed at free Ca^{2+} concentrations of 150 to 750 μM. As compared to rat liver mitochondria, the sensitivity to Ca^{2+} of rat heart mitochondria was much lower in the case of MPTP opening and much higher in the case of respiration inhibition. Naringin, occurring naturally in citrus fruits, partially prevented Ca^{2+}-induced rat cardiac mitochondrial morphological transformations (200 μM), dose-dependently inhibited the respiratory activity of mitochondria (10–75 μM) in the absence or in the presence of calcium ions and promoted membrane potential dissipation and mitochondria swelling in the absence of calcium ions but inhibited calcium-induced MPTP formation at higher concentrations (75 μM).

1. Introduction

The never resting heart is a highly active organ that produces an extraordinary amount of work, requires a high rate of energy flux and a constant supply of metabolic substrates, consumes 10% of the body's total oxygen uptake and makes 35 kg of ATP every day during mitochondrial oxidative phosphorylation (Taegtmeyer 1994). Mitochondria occupy roughly 33% of the cellular volume in each ventricular myocyte (Bers 2001; Bers 2002). This is the largest mitochondrial volume-fraction found in any mammalian cell. To produce energy, the heart muscle mitochondria is known to consume different substrates, fatty acids, glucose, amino acids, pyruvate, lactate, ketone bodies, and even its own constituent proteins. Cardiac mitochondria structural integrity and appropriate functioning are important for normal heart physiology and perturbations in the ability of heart to produce energy or to consume the substrates results in myocardial dysfunctions and cardiovascular disease (Taegtmeyer 1994; Drake et al. 2012; Yu et al. 2022; Williams et al. 2015).

The steady-state mitochondrial Ca^{2+} ($[Ca^{2+}]m$) level is a key regulator of myocardial energy metabolism (Krebs cycle enzymes, an electron transport chain, and F1F0 ATP-synthase), O_2 consumption, proton motive force generation, and ATP production through enhancements in the activities of several mitochondrial substrate transporters and dehydrogenases in myocytes, gene expression and cardiomyocyte growth (Williams et al. 2015; Zhang et al. 2022).

The role of calcium-dependent processes in cardiac physiology and pathophysiology, and *vice versa* the function of mitochondria as a Ca^{2+} buffer and a regulator of calcium homeostasis in cardiac cells have been widely discussed. Impairments in $[Ca^{2+}]$m cycling and mitochondrial network imbalance result in disorders of cellular metabolism and signaling and are the cause of numerous diseases: stroke, heart failure, neurodegeneration, diabetes, and cancer (Carafoli 2002; Gilbert et al. 2020; Garbincius and Elrod 2022; El Hadi et al. 2019).

Induction of the mitochondrial permeability transition pore (MPTP, a high-conductance channel) by Ca^{2+} ions overload and reactive oxygen species (ROS) accumulation can provoke loss of mitochondrial membrane potential and subsequent loss of mitochondrial Ca^{2+}. As shown in the earlier work, this transient opening of the MPTP participates in the development of spontaneous contractions and subsequent ventricular arrhythmia (Bowser et al. 1998).

The molecular machinery that mediates calcium flux across the inner mitochondrial membrane includes a highly selective Ruthenium red (RuR)-sensitive mitochondrial Ca^{2+} uniporter complex (consisting of MCU, EMRE, MICU1, MICU2, MICU3, MCUB, and MCUR1 proteins), the mitochondrial Na^{+}/Ca^{2+} exchanger (NCLX), the mitochondrial H^{+}/Ca^{2+} exchanger (Letm1), the mitochondrial ryanodine receptor, and the MPTP (Garbincius and Elrod 2022; Kirichok et al. 2004; Granatiero et al. 2019). It should be noted that in excitable cells, mitochondria are localized in the vicinity of voltage operated plasma membrane Ca^{2+} channels and can buffer entering Ca^{2+} ions (Santo-Domingo and Demaurex 2010).

Effective heart failure pharmacological therapies appear to lead to mitochondrial dysfunction improvement, regulation of cardiomyocyte calcium homeostasis and prevention of mitochondrial ROS generation (Knowlton et al. 2014; Kumar et al. 2019; Chistiakov et al. 2018). Biologically active natural polyphenolic products, with the flavonoid glycoside naringin being among them, demonstrate high antioxidant, anti-inflammatory, and cardioprotective potential (Rajadurai and Prince 2007). The mechanisms of their biochemical and pharmacological activities are the topics of great interest. In our previous experiments with rat liver mitochondria, we showed stimulation of calcium-induced MPTP formation by the flavonoids naringenin, catechin, and naringin and hypothesized that the effect of the flavonoids on MPTP opening could be mediated by stimulation of the Ca^{2+} uniporter (Zavodnik et al. 2022).

Despite numerous investigations, the details of modulation of mitochondrial and cellular functions in cardiac muscles by Ca^{2+} remain unclear. In the present work, we assessed the mechanism of regulation of MPTP sensitivity, respiratory activity and morphology of isolated rat heart mitochondria under the influence of different concentrations of exogenous Ca^{2+}. Simultaneously, we estimated the efficiency of correction of Ca^{2+}-induced cardiac mitochondria alterations by the polyphenol naringin (flavanone-7-*O*-glycoside) occurring naturally in citrus fruits.

2. Materials and methods

2.1. Chemicals

Calcium chloride dehydrate, succinic acid disodium salt hexahydrate, sucrose, ethylene glycol-bis(β-aminoethyl ether)-N,N,N',N'-tetraacetic acid tetrasodium salt (EGTA), carbonyl cyanide *p*-trifluoromethoxyphenyl hydrazone (FCCP), bovine serum albumin fraction V (BSA), ethylenediaminetetraacetic acid disodium salt (EDTA), 4-(2-Hydroxyethyl)piperazine-1-ethanesulfonic acid, N-(2-Hydroxyethyl)piperazine-N'-(2-ethanesulfonic acid) (HEPES), Araldite 506 Epoxy resin, adenosine 5'-diphosphate sodium salt (ADP), cyclosporin A (CsA), lead citrate, uranyl acetate, Ruthenium red (RuR), naringin (naringenine-7-rhamnosidoglucoside), ethanol, and other chemicals were from Merck / Sigma-Aldrich (St Louis, MO, USA, or Steinheim am Albuch, Germany), osmium tetroxide suitable for electron microscopy was from Carl Roth GmbH (Karlsruhe, Germany). All solutions were made with water purified in the Milli-Q Direct system (Merck KGaA, Darmstadt, Germany). Organic solvents were of analytical grade and used without further purification.

Free calcium concentrations. To determine the effects of calcium ions on mitochondrial functions in the presence of EGTA, added $[Ca^{2+}]$free for a given $[Ca^{2+}]$total was determined using then Ca-EGTA online calculator (https://pcwww.liv.ac.uk/~petesmif/petesmif/software/_webware06/EGTA/EGTA.htm).

2.2. Isolation of rat heart mitochondria

Male albino Wistar rats (200–230 g) were used. The care, use, and all procedures performed were approved by the Ethic Committee of the Institute of Biochemistry of Biologically Active Compounds of the National Academy of Sciences of Belarus (Protocol No 29/20 of 23.05.2020) and complied with the European Convention for the Protection of Vertebrate Animals Used for Experimental and Other Scientific Purposes and the *Guide for the Care and Use of Laboratory Animals* (https://nap.nationalacademies.org/read/12910/chapter/3).

The coupled myocardium mitochondria were isolated from the rat heart by the method of differential centrifugation (Zhang et al. 2022; Johnson and Lardy 1967; Gostimskaya and Galkin 2010). We used the isolation medium containing 0.25 M sucrose, 0.005 M HEPES, 0.0002 M EDTA, and 0.1% BSA, pH 7.4. The isolated heart was quickly transferred into an ice-cold 0.9% KCl solution and carefully washed from the blood. The muscle tissue was weighed, crushed with scissors on ice and homogenized using a glass homogenizer with a Teflon pestle in the isolation medium at 4 ºC. The nuclear fraction was removed by centrifugation at 650 g (10 min, 4 ºC) (a Hermle Z 32 HK centrifuge, Hermle Labortechnik GmbH, Germany). The mitochondria were sedimented by centrifugation at 8 500 g (10 min, 4 ºC) and washed two times in the isolation medium. The pellet of mitochondria was resuspended to an approximate protein concentration of 25–30 mg/ml in the isolation medium. Protein concentrations in myocardium mitochondria were determined by the method of Lowry et al. (1951).

2.3. Electron microscopy of isolated rat heart mitochondria

Rat cardiac muscle mitochondria (5 mg/ml) were exposed to Ca^{2+} ions (550 μM free Ca^{2+}), the flavonoid naringin (200 μM) or Ca^{2+} ions (550 μM free Ca^{2+}) plus the flavonoid naringin (200 μM) in the medium containing 0.25 M sucrose, 0.005 M HEPES, 0.005 M KH_2PO_4 and 0.00005 M EGTA, pH 7.4, for 30 min (26 ºC) *in vitro*. After calcium and flavonoid exposure, the suspensions of mitochondria were centrifuged at 10 000 g, + 4 ºC, for 20 min. Then the mitochondrial pellets were fixed by 2.5% glutaric aldehyde and postfixed in two portions of 1% osmium tetroxide solution in 0.1 M Milloning buffer, pH 7.4 at + 4 ºC for 2 hours (Milloning 1961).

After dehydration by rinsing in alcohols of increasing concentrations and acetone, the samples were embedded in Araldite Epoxy resin. The sections were prepared using a Leica EM UC7 ultramicrotome (Leica Microsystems GmbH, Germany). Semi-thin sections were stained with a 1% solution of methylene blue, whereas ultrathin (35 nm) sections were contrasted with a 2% solution of uranyl acetate and lead citrate by the method of Reynolds (1963) and analyzed with a JEM-1011 electron microscope (Japanese Electron Optics Laboratory Ltd., Japan) at magnifications of 5 000–40 000 and accelerating voltage of 80 kilowatts. Images were captured with an Olympus Mega View III digital camera (Olympus Corporation, Germany) and the iTEM package of programs for treatment of images (Version 5.0, Build 1224, Olympus Corporation, Germany), which has a number of standard built-in algorithms for morphometry. The digital images were used to determine some ultrastructural parameters characterizing the size and shape of these organelles. The morphometric factors were assessed under 20000x or 40000x microscope magnifications on the representative 10 squares (fields of view) tested. Under these magnifications, 250 to 500 mitochondrial profiles were examined. We used 5 animals in each group.

For evaluation of the ultrastructural mitochondrial changes, we used such morphometric parameters as elongation factor, shape factor, and aspect ratio. The elongation factor assesses the lack of roundness of the object (defined as the ratio of the length to the width of the object); as the "ellipsoidality" increases, this parameter raises above 1. Similarly, the shape factor characterizes the "roundness" of the object: this parameter is equal to 1 for the spheres, and for all other shapes it is less than 1. The aspect ratio depends on the ratio of the maximal width and height of the rectangle within which the object is placed.

2.4. Measurements of mitochondrial respiration and membrane potential

Respiration of cardiac mitochondria was measured using an oxygen Clark-type electrode (Hansatech Instruments Limited, Great Britain) in the medium containing 0.25 M sucrose, 0.005 M KH_2PO_4, 0.005 M HEPES, 0.01 M KCl, 0,002 M $MgCl_2$, 0.0002 M EGTA, pH 7.4, at 26 ºC. The mitochondrial suspension (0.5 mg protein/ml) in the respiratory buffer was continuously stirred. To study $FADH_2$-dependent respiration, the oxygen consumption rates were determined in the presence of 5 mM succinate as a substrate (respiratory state 2, V2), after ADP (200 μM) addition (ADP-stimulated state 3, V3) and after ADP consumption (state 4, V4). The respiratory control ratio (RCR) equal to the ratio of the respiratory rates (V3/V4) of mitochondria in state 3 and state 4 and the coefficient of phosphorylation (ADP/O ratio) were calculated.

Mitochondrial membrane potential was detected using a Perkin-Elmer LS55 spectrofluorometer (Great Britain) as the changes in the fluorescent intensity of the dye safranin O (8 μM) at λex/λem 495/586 nm (Akerman and Wikström 1976; Moore and Bonner 1982) in the medium containing 0.25 M sucrose, 0.005 M HEPES, 0.005 M KH_2PO_4, 0.002 M $MgCl_2$, 0.00005 M EGTA, and 5 mM succinate as a substrate, pH 7.4, at 26 °C. Isolated cardiac mitochondria (0.3 mg of protein/ml) were placed into the media and after 5 min effectors were added. The positively charged dye accumulated in mitochondria depending on the mitochondrial membrane potential, resulting in intramitochondrial dye fluorescence quenching. Complete depolarization of mitochondria to calibrate the dye fluorescence was achieved by addition of the uncoupler FCCP (0.5 μM). Membrane potential changes in the presence of calcium ions or naringin were presented as the ratio $(I_{FCCP} – I)/(I_{FCCP} - I_0)$ where I_0 is initial safranin O fluorescence intensity in mitochondrial suspension, I is safranin O fluorescence intensity, I_{FCCP} is safranin O fluorescence intensity after FCCP addition.

2.5. Mitochondrial swelling determination

Ca^{2+}-induced swelling of respiring cardiac mitochondria was measured as we described earlier (Golovach et al. 2017). Briefly, the extent of the mitochondrial permeability transition pore (MPTP) formation was determined from the changes in the optical density of mitochondrial suspension at 540 nm and 26 °C using the buffer containing 0.12 M KCl, 0.005 M HEPES, 0.005 M KH_2PO_4, 0.002 M $MgCl_2$, 0.00005 M EGTA, pH 7.4. Isolated mitochondria (0.5 mg of protein/ml) were added to the medium containing respiratory substrate (5 mM succinate). After 5 min of incubation, Ca^{2+} ions or the flavonoid naringin were added and the rate (ΔD^{540}/min) of the termination phase of swelling was measured, using a Jasco V-650 UV-VIS Spectrophotometer (Japan). At the end of the measurements, the uncoupler FCCP (0.5 μM) was added to the mitochondria to control the completion of the MPTP formation process. To evaluate the effect of cyclosporine A, an inhibitor of MPTP formation, or RuR, an inhibitor of MCU, the mitochondria were pretreated with 1 μM CsA or 10 μM RuR at 26 °C for 3 min.

2.6. Statistics

The data of the experiments, obtained in 5–7 repetitions, were processed statistically by the package of applied program Statistica 10.0 and presented as a median (Me) and an interquartile range between the 25th and the 75th percentile [Q1; Q3]. The normality of distribution was assessed by the Shapiro-Wilk's test. The reliability of differences between the parameters were analyzed using the Mann-Whitney U test and the Kruskal-Wallis H test. The level of significance was considered at $P < 0.05$.

3. Results

3.1. Electron microscopic examination of the effects of exogenous Ca^{2+} ions on heart mitochondria ultrastructure

A typical picture of the ultrastructure of mitochondria isolated from the cardiomyocytes of 3-month-old Wistar rats is presented in Fig. 1. The purity of the mitochondrial fraction made up 90–95% in all the samples studied. In the majority of cases there were few admixtures as small fragments of microfibrils and individual lysosomes and lipofuscin granules. Most of the control mitochondria were of a round shape and distinguished by variable sizes (Fig. 1a). Multiple densely packed cristae occupied all the area of the mitochondrion section and the matrix was of moderate electron density. Such organelles are conventionally classified as those preserving orthodox biosynthetic functional state. Some of the mitochondria had more or less pronounced ultrastructural changes. These organelles were generally distinguished by an irregular shape, a light matrix and a larger size as compared to the majority of the neighboring organelles. It should be noted that control samples displayed only individual mitochondria with pronounced damage.

After exposure to 550 μM free Ca^{2+} ions, we observed appearance of swollen organelles with an electron-light matrix, a larger size, an irregular shape and a damaged native structure of the inner membrane (Fig. 1b). In the setting of the swollen matrix, mitochondria showed the formation of areas completely devoid of cristae, elongation of the intercristae spaces, the cristae lost contacts with the outer wall, were located irregularly and often aggregated on the periphery (Fig. 1b). In this situation, a mitochondrion, with the cristae area being not less than half the total surface area of the section, was classified as the organelle with a moderately disrupted structure, whereas a mitochondrion, with the cristae area being less than half the total square of the section, was classified as the organelle with a substantially impaired structure. Mitochondria with moderately and substantially impaired structures were seen much more frequently in comparison with control. The visual analysis of the ultrastructural transformations was confirmed by morphometrical measurements (Table). The mitochondrial exposure to 550 μM free Ca^{2+} induced an increase in the cross-section area (by 20%), in the average perimeter (by 12%) and in the mean diameter (by 15%) of one mitochondrion. The elongation factor elevated and the organelle sphericity decreased, with the shape factor remaining changed.

The exposure of heart mitochondria to the flavonoid naringin (200 μM) alone induced some visible changes in organelle ultrastructure (Fig. 1d) and affected the morphometrical parameters: increased the average section area (by 10%), the average perimeter of mitochondria, the mean diameter and sphericity, but reduced the aspect ratio and elongation factor (Table). When mitochondria were exposed to Ca^{2+} ions (550 μM free Ca^{2+}) in the presence of naringin (200 μM), we observed prevention of ultrastructural impairments (Fig. 1c, Table). The samples of the mitochondrial fraction of this group showed a greater amount of the organelles with preserved structures as opposed to the group exposed to Ca^{2+} without naringin correction and the majority of the organelles were characterized by a round shape, as in the case of control mitochondria, a matrix of moderate electron density and distinct, random cristae. The mean section area, the mean perimeter, and the mean diameter of mitochondria exposure to Ca^{2+} ions in the presence of naringin were not changed in comparison with control organelles (Table).

Table. Morphometric parameters of isolated rat heart mitochondria before and after treatment by Ca^{2+} ions. Effect of naringin.

Rat cardiac muscle mitochondria (5 mg/ml) were exposure to Ca^{2+} ions (550 μM Ca^{2+} free), flavonoid naringin (200 μM) or Ca^{2+} ions (550 μM Ca^{2+} free) plus flavonoid naringin (200 μM) in the medium containing 0.25 M sucrose, 0.005 M HEPES, 0.005 M KH_2PO_4, 0.00005 M EGTA, pH 7.4, for 30 min (26 ºC) *in vitro*. We used 5 animals in each group. The results were expressed as Me [Q1; Q3].

Morphometric parameters	**Control**	**550 μM Ca^{2+}free**	**550 μM Ca^{2+}free + naringin 200 μM**	**naringin 200 μM**
Area (average section area of one mitochondrion), μm^2	0.62 [0.40;0.89]	0.74 [0.44;1.26]*	0.62 [0.39;0.87]#	0.67 [0.46;1.01]*
Perimeter (average perimeter of one mitochondrion), μm	3.21 [2.55;3.90]	3.60 [2.78; 4.68]*	3.21 [2.56;3.88]*#	3.38 [2.76;4.16]*
Aspect ratio	1.48 [1.36;1.62]	1.59 [1.45; 1.76]*	1.57 [1.45;1.73]*	1.42 [1.32;1.59]*@
Elongation factor	1.48 [1.34;1.61]	1.57 [1.41; 1.73]*	1.56 [1.45;1.74]*	1.42 [1.29;1.59]*@
Mean Gray value (mean relative electron density of mitochondria)	115.4 [106.5;131.0]	147.8 [124.8;161.2]*	129.1 [119.4;147.6]*#	125.1 [108.0;139.3]*@
ECD (equivalent circle diameter), μm	0.89 [0.71;1.07]	0.98 [0.75;1.28]*	0.89 [0.71;1.05]#	0.93 [0.76;1.13]*@
Mean Diameter (average diameter of one mitochondrion), μm	1.01 [0.79;1.22]	1.14 [0.85;1.49]*	1.01 [0.79;1.25]#	1.07 [0.88;1.29]*@
Sphericity	0.46 [0.38;0.55]	0.41 [0.34;0.50]*	0.42 [0.34;0.49]*	0.52 [0.41;0.61]*@
Shape Factor	0.78 [0.72;0.82]	0.77 [0.70;0.81]	0.77 [0.71;0.80]	0.78 [0.71;0.82]
* - $p < 0.05$ in comparison with Control				
# - $p < 0.05$ in comparison with 550 μM Ca^{2+} free				
@ - $p < 0.05$ in comparison with 550 μM Ca^{2+} free + naringin 200 μM				

3.2. Respiratory parameters of rat heart mitochondria in vitro in the presence of Ca^{2+} ions. Effect of plant polyphenol.

In the next step of our *in vitro* experiments, we evaluated the effects of Ca^{2+} ions and the flavonoid naringin on the parameters of mitochondrial respiration. The low concentrations of exogenous free Ca^{2+} ions (we used the 0.0002 M EGTA-containing medium and the calculated Ca^{2+} free concentrations were of 20 to 250 nM) dose-dependently inhibited the substrate-stimulated oxygen consumption rate V2 and the ADP-dependent oxygen consumption rate V3. The coefficient RCR and the coefficient of phosphorylation ADP/O were not considerably changed (Figs. 2a, b)

Taking into consideration the possibility of plant polyphenols to influence mitochondrial activity, we studied the modulatory effects of the flavonoid naringin, widely distributed in the human diet, on the respiratory parameters of isolated rat cardiac mitochondria in the absence or in the presence of calcium ions (Ca^{2+}free = 240 nM) *in vitro*. In the absence or in the presence of Ca^{2+} ions, naringin (10–75 μM) dose-dependently diminished the ADP-stimulated oxygen-consumption rate V3 in mitochondria (Fig. 3a). Flavonoid increased oxygen-consumption rate V2 in the absence of Ca^{2+} and decrease this parameter in the presence of Ca^{2+} (Fig. 3a), as well as decreased the coefficient RCR (V4/V3), but did not influence the coefficient ADP/O (Fig. 3b).

3.3. Heart mitochondria permeability transition and membrane depolarization induced by Ca^{2+} ions and naringin in vitro

Further we compared the effect of Ca^{2+} ions on respiratory parameters of cardiac mitochondria with those on swelling and membrane potential of cardiac mitochondria energized by succinate. The rate of MPTP formation was measured using the initial part of the kinetic curves of Ca^{2+}-induced mitochondrial swelling. Figures 4a and 4b show representative tracks of rat heart mitochondrial swelling as a result of MPTP opening that was recorded by changing the intensity of mitochondrial suspension light scattering (D^{540}) in the presence of increasing concentrations of Ca^{2+} ions.

As one can see, the apparent rate of MPTP formation dose-dependently increased in the presence of calcium ions (Figs. 4, 5). CsA, a known inhibitor of MPTP opening, completely prevented heart mitochondria swelling (Fig. 4a). Simultaneously, the higher concentrations of the calcium chelator EGTA (0.0005 M) also prevented Ca^{2+}-induced MPTP opening (Fig. 4a). The specific inhibitor of MCU, RuR, completely inhibited Ca^{2+}-induced mitochondria swelling as well (Fig. 4b). The polyphenolic effector naringin (25–75 μM) promoted mitochondria swelling in the absence of calcium ions (Figs. 4b, 6), but inhibited calcium-induced MPTP formation at higher concentrations (75 μM).
Figs. 7a and 7b show representative traces of the probe safranin O fluorescence intensity changes after mitochondria exposure to Ca^{2+} ions or naringin. Ca^{2+} ions (Ca^{2+}free = 100 – 550 μM) effectively dissipated mitochondrial membrane potential in the EGTA-containing media. Simultaneously, the heart

mitochondria exposure to naringin (75 μM) resulted in dissipation of membrane potential in the absence of Ca^{2+} (Fig. 7). RuR prevented Ca^{2+}-induced dissipation of cardiac mitochondria membrane potential in the absence (completely) or in the presence of naringin (partially) (Fig. 7).

4. Discussion

Ca^{2+} signaling pathways play fundamental roles in the heart as regulators of the contractile function and cardiomyocyte growth, and altered Ca^{2+} homeostasis is the main cause of cardiovascular diseases (Gilbert et al. 2020). In the earlier work of Miyamae et al., it was shown that cardiac mitochondrial Ca^{2+} was in the range of 0.1–0.2 μM, and elevated to a higher steady-state level during increasing beating frequency (Miyamae et al. 1996). The cardiomyocyte possesses spatially separated populations of mitochondria which respond to pathological conditions heterogeneously (Rosca et al. 2008). Subsarcolemmal mitochondria (SSM) exist below the sarcolemma, interfibrillar mitochondria (IFM) reside in the rows between the myofibril contractile apparatus, and perinuclear mitochondria are situated at the nuclear poles in the perinuclear region (Hollander et al. 2014; Shimada et al. 1984). As was shown earlier electron transport chain complex activities do not differ significantly in IFM and SSM (Rosca et al. 2008). Using scanning electron microscopy earlier it was shown that interfibrillar mitochondria were elongated and usually about the same length as the sarcomere and that subsarcolemmal mitochondria varied in size and shape, being rod-like, spherical, polygonal or horseshoe-like (Shimada et al. 1984).

In our experiment, the ultrastructure of the control cardiac rat mitochondria corresponded to the optimal bioenergetic potential. Overload by calcium ions (free Ca^{2+} concentration was 550 μM) showed a dramatic increase in mitochondrial heterogeneity in size and electron density. The swollen mitochondria in the presence of Ca^{2+} were characterized by lowered bioenergetic and biosynthetic potentials.

Our results demonstrated an influence of naringin alone on the isolated heart mitochondria ultrastructure. In our work, naringin influenced mitochondrial functions and affected the response of the rat heart mitochondria to Ca^{2+} ions: the preliminary exposure of mitochondria to naringin partially prevented Ca^{2+} ion-induced structural transformations, naringin dose-dependently inhibited mitochondrial oxygen consumption, stimulated MPTP opening and membrane depolarization in the absence of Ca^{2+} (this fact correlated with the morphological transformations of mitochondria observed in the presence of naringin), but partially prevented Ca^{2+}-induced MPTP opening (25–100 μM). The decrease in membrane potential by naringin probably diminished potential-dependent calcium ion accumulation by mitochondria. In our experiment, RuR, a specific inhibitor of mitochondrial calcium uniporter, completely inhibited Ca^{2+}-dependent membrane depolarization, but did not affect markedly the stimulation of these processes by naringin. Therefore, one can suggest, that naringin stimulate mitochondrial membrane Ca^{2+}- permeability. The uncoupling effect of the flavonoids and their ability to dissipate mitochondrial membrane potential have been attributed to weak-acidic and hydrophobic nature of the flavonoids [Sandoval-Acuña et al. 2014].

Previously, for rat liver mitochondria we suggested a direct incorporation of the flavonoids, quercetin, catechin and naringenin, in the mitochondrial membrane and a change in membrane stability, as well as an effect of the flavonoids as proton/calcium ions carriers and Ca^{2+} ions chelators (Veiko et al. 2020). It is well known that a large number of plant flavonoids are capable of forming stable metal complexes through their multiple OH groups and the carbonyl moiety and of preventing the toxicity of active metal ions (Cherrak et al. 2016). The reactive polyphenols can act as either agonists or antagonists of MPTP opening depending on the experimental conditions and polyphenol concentrations (Ortega and García 2009; Marchi et al. 2009). One of the main results of the mitochondrial calcium overload is the MPTP formation resulting in Ca^{2+} linked necrotic and apoptotic (or necroapoptotic) myocyte death (Lemasters et al. 2009). We suggested that the Ca^{2+}-induced ultrastructural disturbances in rat heart mitochondria and mitochondrial membrane depolarization, were probably a result of MPTP opening (free Ca^{2+}concentrations were 150–750 μM) (Fig. 5) and the changes in the mitochondrial respiratory activity were not related to the MPTP formations.

Using the Lineweaver-Burk plot of the dependence of the reciprocal apparent swelling rate ($min/\Delta D^{540}$) on the reciprocal Ca^{2+} concentration ($1/[Ca^{2+}]$), we calculated the apparent Michaelis-Menten constant, K_m, of Ca^{2+} ions interaction with rat cardiac mitochondria sites (or Ca^{2+} concentration corresponding to half the maximal swelling rate) (Fig. 5b). The apparent K_m of the MPTP formation for cardiac mitochondria was calculated to be 350 ± 50 μM. Earlier it was shown that the cardiac MCU conductance is assumed to follow a Michaelis-Menten type relationship with a K_m of 19 mM Ca^{2+} (Williams et al. 2013). For comparison, the apparent K_m for MPTP formation in the isolated rat liver mitochondria was previously calculated to be 75 ± 20 μM (Golovach et al. 2017). Bernardi has recently suggested at least two pathways for Ca^{2+}-dependent mitochondria permeabilization: 1) high-conductance F-ATP synthase-dependent MPTP opening, which is inhibited by CsA, but not by bongkrekate (BKA), and 2) adenine nucleotide translocase (ANT) dependent MPTP opening, which is inhibited by both CsA and BKA (Bernardi 2020). Halestrap et al. suggested the MPTP to be a promising drug target in human cardiovascular disease (Halestrap and Pasdois 2009).

According to our results, low free Ca^{2+} concentrations (40–250 nM) effectively inhibited the respiratory activity of rat heart mitochondria, remaining unaffected the coefficient ADP/O. Inhibition of the respiratory activity of heart mitochondria preceded Ca^{2+}-linked MPTP or membrane depolarization.

Biphasic Ca^{2+} effects such as small increases in Ca^{2+} concentration stimulating mitochondrial respiration and considerable Ca^{2+} elevations inhibiting respiration were detected both in heart and kidney mitochondria (Zhang et al. 2022; Anmann et al. 2005). The sensitivity of O_2 utilization and ATP synthesis to Ca^{2+} ions were substrate-dependent and organ (heart and kidney) – specific (Zhang et al. 2022). Similarly, using isolated mice skeletal muscle mitochondria energized by the complex I substrates, glutamate/malate (not succinate), Fink et al. showed that free Ca^{2+}at 450 nM enhanced respiration and ATP production, but inhibited these processes at 10 μM or higher concentrations (Fink et al. 2017).

We observed earlier that the MPTP opening in rat liver mitochondria caused ultrastructural disturbances, effective inhibition of respiratory activity, uncoupling respiration and oxidation processes, as well as mitochondrial potential dissipation in the presence of lower concentrations of exogenous Ca^{2+} (20–60 μM) (Zavodnik et al. 2022; Golovach et al. 2017) compared to heart mitochondria. The susceptibility of cardiac mitochondria to calcium-induced MPTP opening was much lower, but the susceptibility of mitochondrial respiration was much higher in comparison with liver mitochondria. Similarly, Drahota and coauthors demonstrated earlier that as compared to liver mitochondria, the MPTP of cardiac mitochondria were more resistant to damaging effects of the calcium load and oxidative stress (Drahota et al. 2012).

Conclusions

Our present findings point out that the low concentrations of exogenous free Ca^{2+} ions (calculated Ca^{2+}free concentrations were of 40 to 250 nM) dose-dependently inhibited the succinate-stimulated oxygen consumption rate V2 and the ADP-dependent oxygen consumption rate V3 without significant changes in the coefficients RCR and ADP/O. The high exogenous Ca^{2+} ion concentrations (the free Ca^{2+} concentration was 550 μM) promoted a dramatic increase in mitochondrial heterogeneity in size and electron density due to the occurrence of swollen organelles with an electron-light matrix, a larger size, an irregular shape, elongation of the intercristae spaces, and a damaged native structure of the inner membrane of rat heart mitochondria. The ultrastructural disturbances in heart mitochondria were connected with calcium-induced opening of the MPTP and membrane depolarization, observed at free Ca^{2+} concentrations of 150 to 750 μM. Using the Lineweaver-Burk plot of the dependence of the reciprocal apparent swelling rate ($min/\Delta D^{540}$) on the reciprocal Ca^{2+} concentration ($1/[Ca^{2+}]$), we calculated the apparent Michaelis-Menten constant of Ca^{2+} ions interaction with rat cardiac mitochondria sites, K_m= 350 ± 50 μM. As compared to liver mitochondria, the sensitivity to Ca^{2+} of rat heart mitochondria was much lower in the case of MPTP opening and much higher in the case of respiration inhibition. The preliminary exposure of cardiac mitochondria to the flavonoid naringin alone affected the morphometrical parameters (200 μM): increased the average section area and the perimeter of mitochondria, stimulated mitochondria swelling and membrane potential loss (25–100 μM) in the absence of Ca^{2+}, partially prevented Ca^{2+} ion- induced morphological transformations (200 μM) in mitochondria, dose-dependently (25–75 μM) diminished the oxygen-consumption rates V3 and V2 in the absence or in the presence of Ca^{2+} ions, as well as inhibited Ca^{2+} ion-stimulated MPTP opening. These effects of weak-acidic and lipophilic naringin could be explained due to a direct interaction of naringin with isolated mitochondria, its protonophoric/ionophoric properties. One can suggest that the decrease in membrane potential by naringin diminishes the potential-dependent accumulation of calcium ions by mitochondria.

Abbreviations

ADP – adenosine 5'-diphosphate sodium salt, ANT – adenine nucleotide translocase, BKA – bongkrekate, BSA – bovine serum albumin, CsA – cyclosporine A, EDTA – ethylenediaminetetraacetic acid disodium salt, EGTA – ethylene glycol-bis(β-aminoethyl ether)-N,N,N',N'-tetraacetic acid tetrasodium salt, ER/SR – endoplasmic/sarcoplasmic reticulum, FCCP – carbonyl cyanide 4-(trifluoromethoxy)phenylhydrazone, HEPES – 4-(2-Hydroxyethyl)piperazine-1-ethanesulfonic acid, N-(2-Hydroxyethyl)piperazine-N'-(2-ethanesulfonic acid), IFM – interfibrillar mitochondria, MAMs – mitochondria associated membranes, Me – median, MCU - mitochondrial Ca^{2+} uniporter, MPTP – mitochondrial permeability transition pore, PBS – isotonic buffered saline, RCR – respiratory control ratio, ROS – reactive oxygen species, RuR – Ruthenium red, SERCA – sarcoplasmic reticulum Ca^{2+}-ATPase, SSM – subsarcolemmal mitochondria

Declarations

Conflict of Interest: The authors declare no conflicts of interest.

Informed consent: Informed written consent was obtained from all the individual participants included in the study.

Acknowledgments

This study was partially supported by grant No M23KI – 14 for joint scientific projects from the Belarusian Republican Foundation for Fundamental Research – National Scientific Foundation of China

CRediT author statement

T.A. Kavalenia: investigation, data curation, software, E.A. Lapshina: data curation, validation, software, writing-original draft preparation, T.V. Ilyich: investigation, software, visualization, Hu-Cheng Zhao: conceptualization, methodology, supervision, I.B. Zavodnik: conceptualization, writing-reviewing and editing.

All the authors approved the final version of the manuscript.

References

1. Akerman KE, Wikström MK (1976) Safranine as a probe of the mitochondrial membrane potential. FEBS Lett 68:191-197. https://doi.org/10.1016/0014-5793(76)80434-6
2. Anmann T, Eimre M, Kuznetsov AV, Andrienko T, Kaambre T, Sikk P, Seppet E, Tiivel T, Vendelin M, Seppet E, Saks VA (2005) Calcium-induced contraction of sarcomeres changes the regulation of mitochondrial respiration in permeabilized cardiac cells. FEBS J 272:3145-3161. https://doi.org/10.1111/j.1742-4658.2005.04734.x
3. Bernardi P (2020) Mechanisms for Ca^{2+}-dependent permeability transition in mitochondria. Proc Natl Acad Sci USA 117:2743-2744. https://doi.org/10.1073/pnas.1921035117
4. Bers DM (2001) Excitation-contraction coupling and cardiac contractile force. Springer, Dordrecht

5. Bers DM (2002) Cardiac excitation-contraction coupling. Nature 415:198-205. https://doi.org/10.1038/415198a
6. Bowser DN, Minamikawa T, Nagley P, Williams DA (1998) Role of mitochondria in calcium regulation of spontaneously contracting cardiac muscle cells. Biophys J 75:2004-2014. https://doi.org/10.1016/S0006-3495(98)77642-8
7. Carafoli E (2002) Calcium signaling: a tale for all seasons. Proc Natl Acad Sci USA 99:1115-1122. https://doi.org/10.1073/pnas.032427999
8. Cherrak SA, Mokhtari-Soulimane N, Berroukeche F, Bensenane B, Cherbonnel A, Merzouk H, Elhabiri M (2016) *In vitro* antioxidant *versus* metal ion chelating properties of flavonoids: a structure-activity investigation. PLoS One 11:e0165575. https://doi.org/10.1371/journal.pone.0165575
9. Chistiakov DA, Shkurat TP, Melnichenko AA, Grechko AV, Orekhov AN (2018) The role of mitochondrial dysfunction in cardiovascular disease: a brief review. Ann Med 50:121-127. https://doi.org/10.1080/07853890.2017.1417631
10. De Marchi U, Biasutto L, Garbisa S, Toninello A, Zoratti M (2009) Quercetin can act either as an inhibitor or an inducer of the mitochondrial permeability transition pore: a demonstration of the ambivalent redox character of polyphenols. Biochim Biophys Acta 1787:1425-1432. https://doi.org/10.1016/j.bbabio.2009.06.002
11. Drahota Z, Milerová M, Endlicher R, Rychtrmoc D, Červinková Z, Ošťádal B (2012) Developmental changes of the sensitivity of cardiac and liver mitochondrial permeability transition pore to calcium load and oxidative stress. Physiol Res 61:S165-S172. https://doi.org/10.33549/physiolres.932377
12. Drake KJ, Sidorov VY, McGuinness OP, Wasserman DH, Wikswo JP (2012) Amino acids as metabolic substrates during cardiac ischemia. Exp Biol Med 237:1369-1378. https://doi.org/10.1258/ebm.2012.012025
13. EGTA - Version 2.0 HTML/Javascript by PeteSmif. https://pcwww.liv.ac.uk/~petesmif/petesmif/software/_webware06/EGTA/EGTA.htm. Accessed 13 January 2023
14. El Hadi H, Vettor R, Rossato M (2019) Cardiomyocyte mitochondrial dysfunction in diabetes and its contribution in cardiac arrhythmogenesis. Mitochondrion 46:6-14. https://doi.org/10.1016/j.mito.2019.03.005
15. Fink BD, Bai F, Yu L, Sivitz WI (2017) Regulation of ATP production: dependence on calcium concentration and respiratory state. Am J Physiol Cell Physiol 313:C146-C153. https://doi.org/10.1152/ajpcell.00086.2017
16. Garbincius JF, Elrod JW (2022) Mitochondrial calcium exchange in physiology and disease. Physiol Rev 102:893-992. https://doi.org/10.1152/physrev.00041.2020
17. Gilbert G, Demydenko K, Dries E, Puertas RD, Jin X, Sipido K, Roderick HL (2020) Calcium signaling in cardiomyocyte function. Cold Spring Harb Perspect Biol 12:a035428. https://doi.org/10.1101/cshperspect.a035428

18. Golovach NG, Cheshchevik VT, Lapshina EA, Ilyich TV, Zavodnik IB (2017) Calcium-induced mitochondrial permeability transitions: parameters of Ca^{2+} ion interactions with mitochondria and effects of oxidative agents. J Membr Biol 250:225-236. https://doi.org/10.1007/s00232-017-9953-2
19. Gostimskaya I, Galkin A (2010) Preparation of highly coupled rat heart mitochondria. J Vis Exp 23:2202. https://doi.org/10.3791/2202
20. Granatiero V, Pacifici M, Raffaello A, De Stefani D, Rizzuto R (2019) Overexpression of mitochondrial calcium uniporter causes neuronal death. Oxid Med Cell Longev 2019:1681254. https://doi.org/10.1155/2019/1681254
21. Halestrap AP, Pasdois P (2009) The role of the mitochondrial permeability transition pore in heart disease. Biochim Biophys Acta 1787:1402-1415. https://doi.org/10.1016/j.bbabio.2008.12.017
22. Hollander JM, Thapa D, Shepherd DL (2014) Physiological and structural differences in spatially distinct subpopulations of cardiac mitochondria: influence of cardiac pathologies. Am J Physiol Heart Circ Physiol 307:H1–H14. https://doi.org/10.1152/ajpheart.00747.2013
23. Johnson D, Lardy HA (1967) Isolation of liver or kidney mitochondria. Meth Enzymol 10:94-101.
24. Kirichok Y, Krapivinsky G, Clapham DE (2004) The mitochondrial calcium uniporter is a highly selective ion channel. Nature 427:360-364. https://doi.org/10.1038/nature02246
25. Knowlton AA, Chen L, Malik ZA (2014) Heart failure and mitochondrial dysfunction: the role of mitochondrial fission/fusion abnormalities and new therapeutic strategies. J Cardiovasc Pharmacol 63:196-206. https://doi.org/10.1097/01.fjc.0000432861.55968.a6
26. Kumar AA, Kelly DP, Chirinos JA (2019) Mitochondrial dysfunction in heart failure with preserved ejection fraction. Circulation 139:1435-1450. https://doi.org/10.1161/CIRCULATIONAHA.118.036259
27. Lemasters JJ, Theruvath TP, Zhong Z, Nieminen A-L (2009) Mitochondrial calcium and the permeability transition in cell death. Biochim Biophys Acta 1787:1395-1401. https://doi.org/10.1016/j.bbabio.2009.06.009
28. Lowry OH, Rosebrough NJ, Farr AL, Randall RJ (1951) Protein measurement with the Folin phenol reagent. J Biol Chem 193:265-275. https://doi.org/10.1016/s0021-9258(19)52451-6
29. Millonig GA (1961) Advantages of a phosphate buffer for osmium tetroxide solutions in fixation. J Appl Physics 32:1637-1643.
30. Miyamae M, Camacho SA, Weiner MW, Figueredo VM (1996) Attenuation of postischemic reperfusion injury is related to prevention of $[Ca^{2+}]$m overload in rat hearts. Am J Physiol 271:H2145–H2153. https://doi.org/10.1152/ajpheart.1996.271.5.H2145
31. Moore AL, Bonner WD (1982) Measurements of membrane potentials in plant mitochondria with the safranine method. Plant Physiol 70:1271-1276. https://doi.org/10.1104/pp.70.5.1271
32. National Research Council (US) (2011) Guide for the Care and Use of Laboratory Animals. National Academies Press (US), Washington (DC)
33. Ortega R, García N (2009) The flavonoid quercetin induces changes in mitochondrial permeability by inhibiting adenine nucleotide translocase. J Bioenerg Biomembr 41:41-47.

https://doi.org/10.1007/s10863-009-9198-6

34. Rajadurai M, Prince PSM (2007) Preventive effect of naringin on cardiac mitochondrial enzymes during isoproterenol-induced myocardial infarction in rats: a transmission electron microscopic study. J Biochem Mol Toxicol 21:354-631. https://doi.org/10.1002/jbt.20203
35. Reynolds ES (1963) The use of lead citrate at high pH as an electron opaque stain in electron microscopy. J Cell Biol 17:208-212. https://doi.org/10.1083/jcb.17.1.208
36. Rosca MG, Vazquez EJ, Kerner J, Parland W, Chandler MP, Stanley W, Sabbah HN, Hoppel CL (2008) Cardiac mitochondria in heart failure: decrease in respirasomes and oxidative phosphorylation. Cardiovasc Res 80:30-39. https://doi.org/10.1093/cvr/cvn184
37. C. Sandoval-Acuña Shimada et al., J. Ferreira, H. Speisky, Polyphenols and mitochondria: An update on their increasingly emerging ROS-scavenging independent actions, Arch. Biochem. Biophys., Vol. 559, 2014, P. 75-90, doi.org/10.1016/j.abb.2014.05.017
38. Santo-Domingo J, Demaurex N (2010) Calcium uptake mechanisms of mitochondria. Biochim Biophys Acta 1797:907-912. https://doi.org/10.1016/j.bbabio.2010.01.005
39. Shimada T, Horita K, Murakami M, Ogura R (1984) Morphological studies of different mitochondrial populations in monkey myocardial cells. Cell Tissue Res 238:577-582. http://doi.org/10.1007/BF00219874
40. Taegtmeyer H (1994) Energy metabolism of the heart: from basic concepts to clinical applications. Curr Probl Cardiol 19:59-113. https://doi.org/10.1016/0146-2806(94)90008-6
41. Veiko AG, Sekowski S, Lapshina EA, Wilczewska AZ, Markiewicz KH, Zamaraeva M, Zhao Hu-cheng, Zavodnik IB (2020) Flavonoids modulate liposomal membrane structure, regulate mitochondrial membrane permeability and prevent erythrocyte oxidative damage. Biochim Biophys Acta 1862:183442. https://doi.org/10.1016/j.bbamem.2020.183442
42. Williams GSB, Boyman L, Lederer WJ (2015) Mitochondrial calcium and the regulation of metabolism in the heart. J Mol Cell Cardiol 78:35-45. https://doi.org/10.1016/j.yjmcc.2014.10.019
43. Williams GS, Boyman L, Chikando AC, Khairallah RJ, Lederer WJ (2013) Mitochondrial calcium uptake. Proc Natl Acad Sci USA 110:10479-10486. https://doi.org/10.1073/pnas.1300410110
44. Yu F, McLean B, Badiwala M, Billia F (2022) Heart failure and drug therapies: a metabolic review. Int J Mol Sci 23:2960. https://doi.org/10.3390/ijms23062960
45. Zavodnik IB, Kovalenia TA, Veiko AG, Lapshina EA, Ilyich TV, Kravchuk RI, Zavodnik LB, Klimovich II (2022) Structural and functional changes in rat liver mitochondria under calcium ion loading in the absence and presence of flavonoids. Biomed Khim 68:237-249. https://doi.org/10.18097/PBMC20226804237
46. Zhang X, Tomar N, Kandel SM, Audi SH, Cowley AW Jr, Dash RK (2022) Substrate- and calcium-dependent differential regulation of mitochondrial oxidative phosphorylation and energy production in the heart and kidney. Cells 11:131. https://doi.org/10.3390/cells11010131

Figures

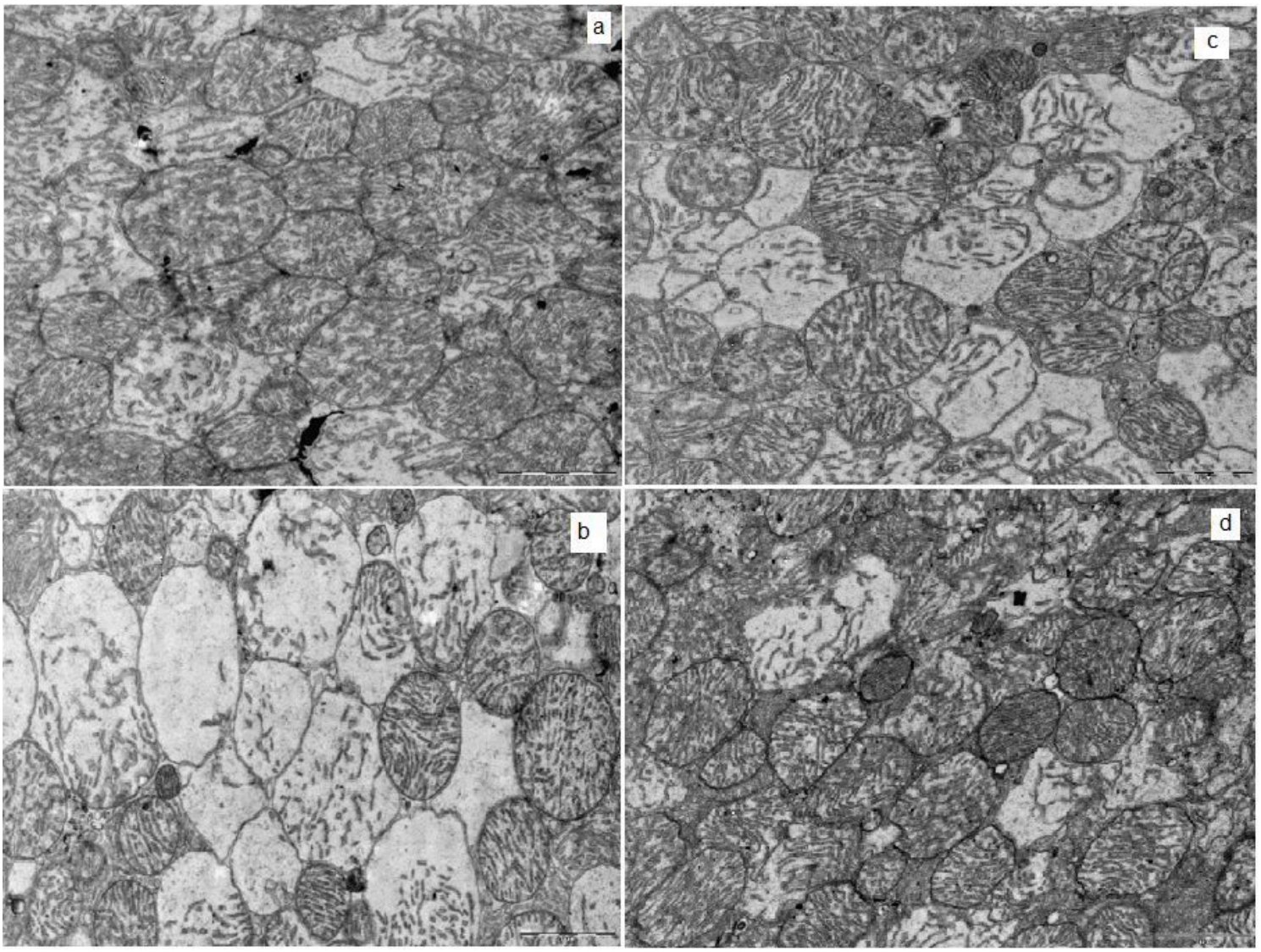

Figure 1

Electron micrographs of isolated rat heart mitochondria:

a) control rat heart mitochondria, b) Ca^{2+}-induced morphological transformations of cardiac mitochondria *in vitro* (Ca^{2+} free = 550 μM, 30 min, 26 ºC), c) heart mitochondria exposed to Ca^{2+} ions (550 μM free Ca^{2+}) in the presence of naringin (200 μM, 30 min, 26 ºC), d) mitochondria exposed to the flavonoid naringin (200 μM, 30 min, 26 ºC). 0.25 M sucrose, 0.005 M HEPES, 0.005 M KH_2PO_4, 0.00005 M EGTA, pH 7.4, x40 000. The scale intervals are equal to 1.0 μm.

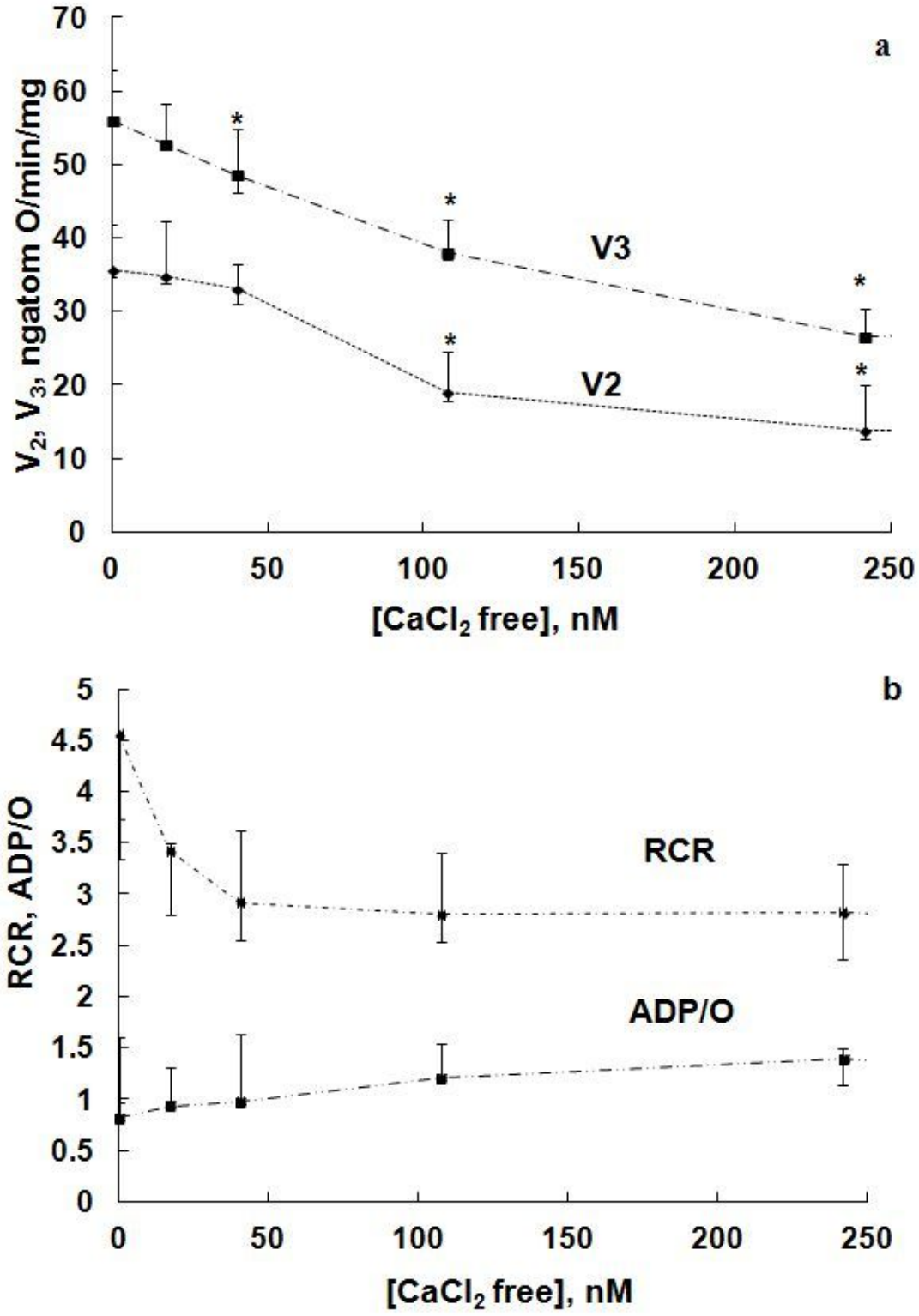

Figure 2

Ca^{2+} ions inhibit respiratory activity of rat heart mitochondria: dependences on Ca^{2+} ion concentrations of the oxygen consumption rate V2, the ADP-dependent oxygen consumption rate V3 (a), and the coefficients RCR and ADP/O (b). Rat heart mitochondria (0.5 mg/ml) were placed in EGTA-containing medium: 0.25 M sucrose, 0.005 M KH_2PO_4, 0.005 M HEPES, 0.01 M KCl, 0,002 M $MgCl_2$, 0.0002 M EGTA, pH 7.4, at 26 ºC. 5 mM succinate as a substrate and 200 μM ADP were added.

Significant difference (P<0.05): **vs.* that in the absence of calcium ions.

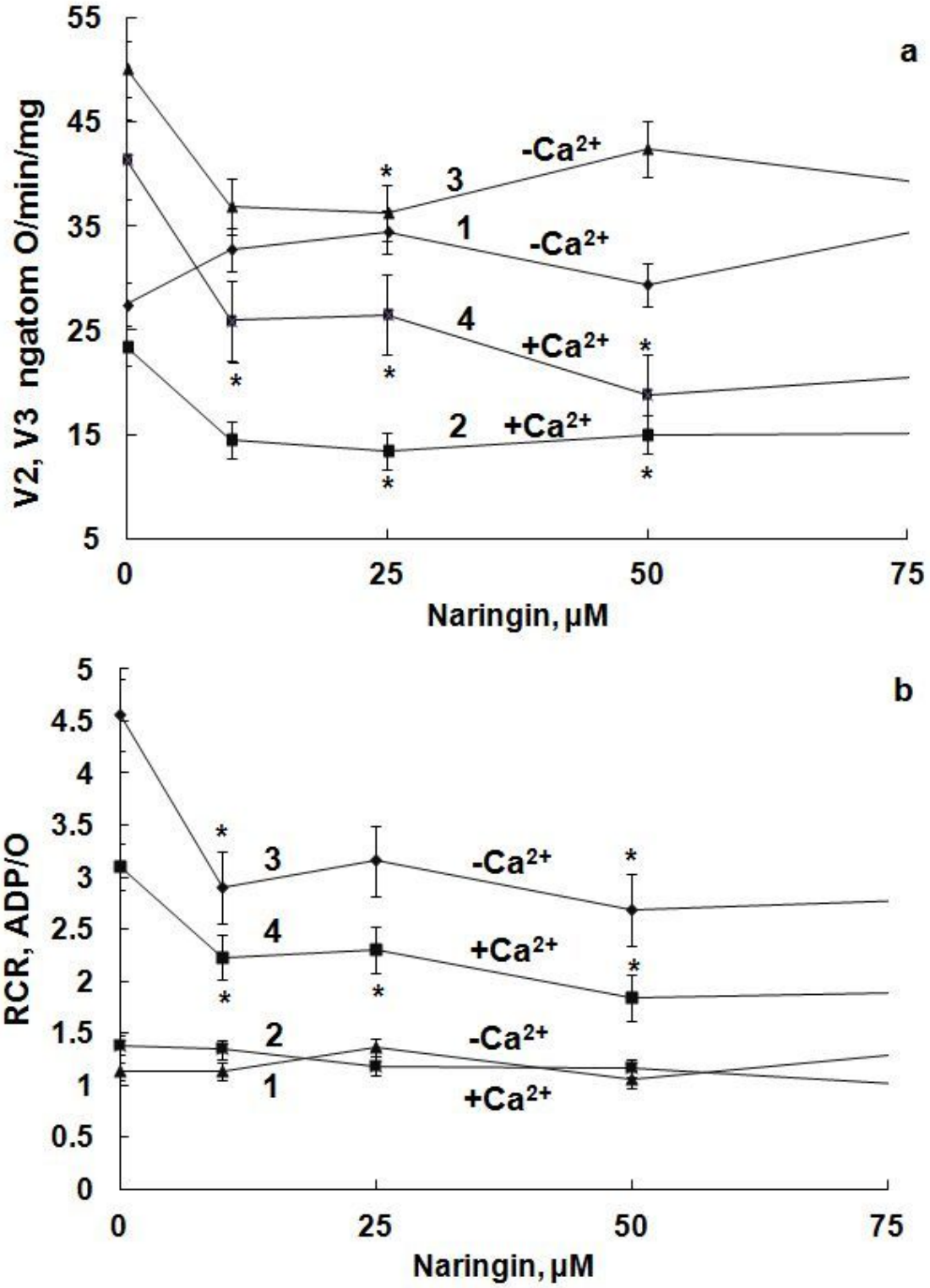

Figure 3

Effect of naringin on the respiration parameters of isolated rat heart mitochondria: (a) the oxygen consumption rates V2 (1, 2) and V3 (3, 4); (b) the coefficient of phosphorylation (ADP/O ratio) (1, 2) and the respiratory control ratio (RCR) (3, 4) in the absence (1, 3) or in the presence of Ca^{2+} ions (Ca^{2+} free =

240 nM) (2, 4). Mitochondria (0.5 mg protein/ml) were placed in the medium containing 0.25 M sucrose, 0.005 M KH_2PO_4, 0.005 M HEPES, 0.01 M KCl, 0,002 M $MgCl_2$, 0.0002 M EGTA, pH 7.4, at 26 ºC, in the absence or in the presence of naringin. 5 mM succinate as a substrate and 200 μM ADP were added.

Significant difference (P<0.05): **vs.* that in the absence of naringin.

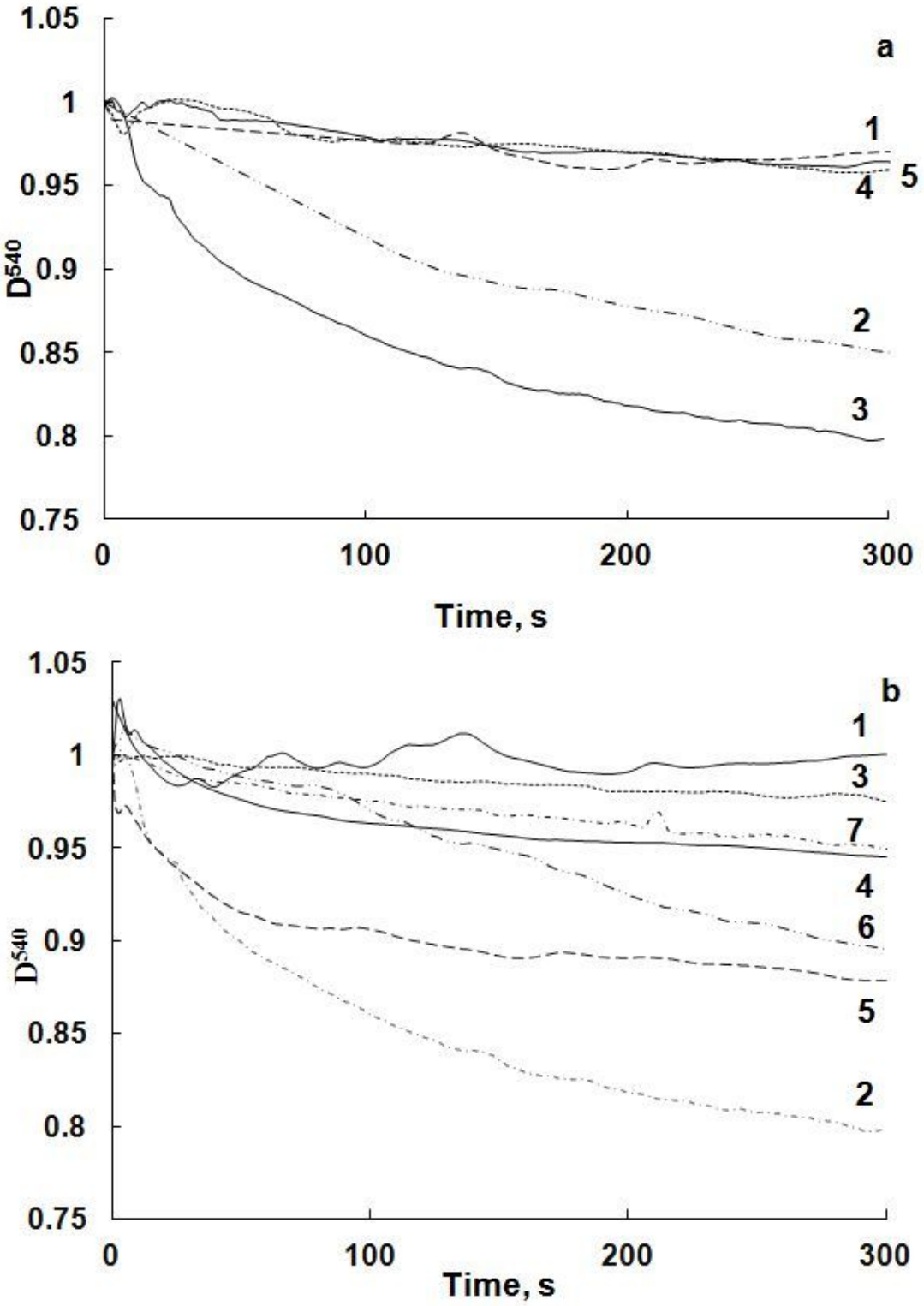

Figure 4

Representative traces of time-dependences of exogenous Ca^{2+}-induced MPTP formations measured as changing optical density (D^{540}) of cardiac mitochondrial suspension at 540 nm: a) in the absence (1, control) and in the presence of exogenous free Ca^{2+}ions: 350 mM (2), 550 mM (600 mM total Ca^{2+}ions) (3), 58 mM (600 mM total Ca^{2+} ions in the presence of 0.0005 M EGTA) (4), 550 mM free Ca^{2+}+10 mM RuR (5);

b) in the absence (1, control) and in the presence of exogenous free Ca^{2+} ions and naringin: free Ca^{2+} 550 mM (2), free Ca^{2+} 550 mM + 1 mM CsA (3), naringin 25 mM (4), naringin 100 mM (5), free Ca^{2+} 550 mM + naringin 75 mM (6), free Ca^{2+} 550 mM + naringin 75 mM + 10 mM RuR (7).
0.12 M KCl, 0.005 M HEPES, 0.005 M KH_2PO_4, 0.002 M $MgCl_2$, and 0.00005 M EGTA, pH 7.4 at 26 ºC, 5 mM succinate as a substrate, 0.5 mg protein/ml.

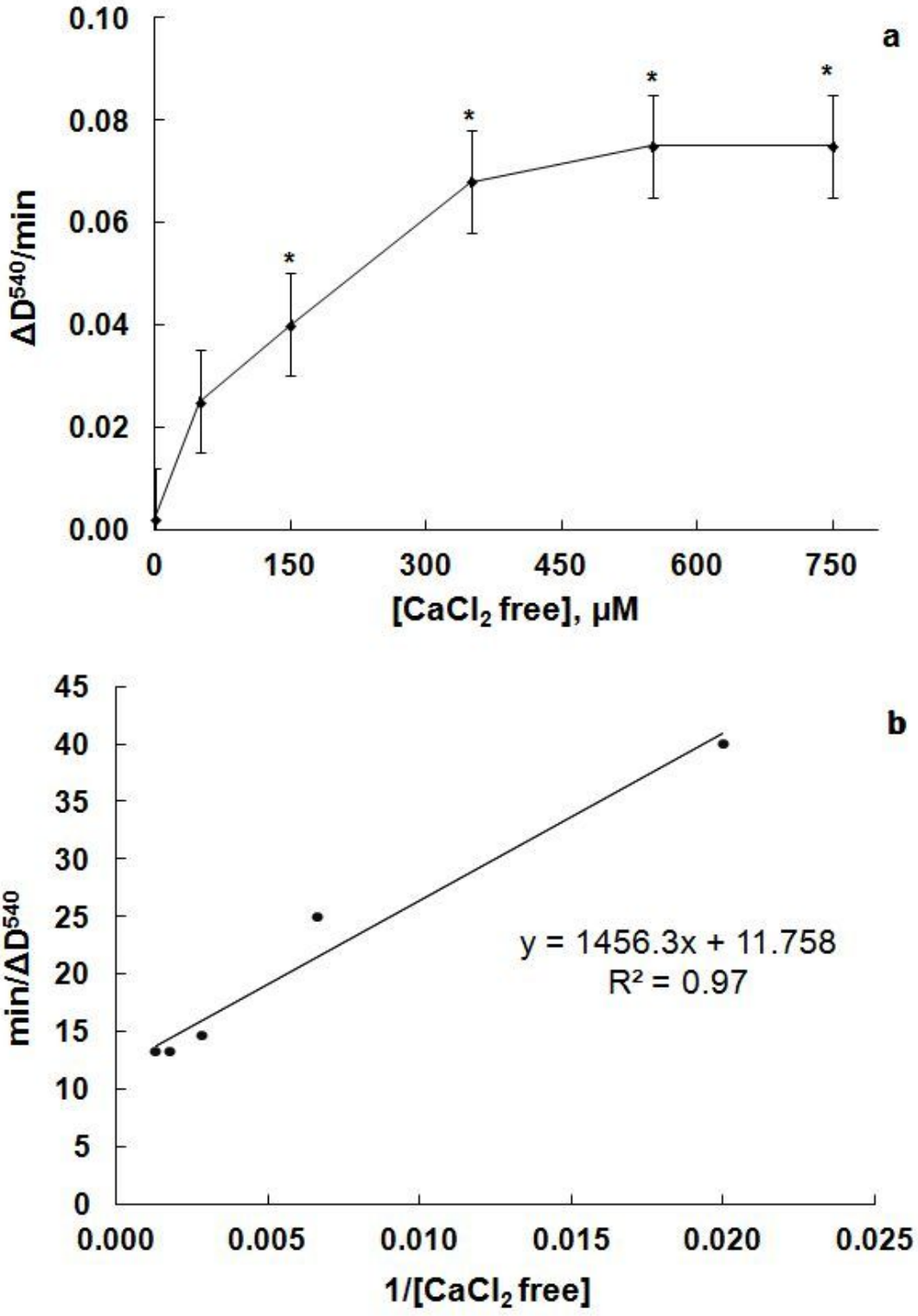

Figure 5

a) Effect of free Ca^{2+} ion concentrations on the rate of MPTP (ΔD^{540}/min) formation for rat heart mitochondria, b) the same dependence represented as the Lineweaver-Burk plot (or a double reciprocal plot).

0.12 M KCl, 0.005 M HEPES, 0.005 M KH_2PO_4, 0.002 M $MgCl_2$, and 0.00005 M EGTA, pH 7.4 at 26 ºC, 5 mM succinate as a substrate, 0.5 mg protein/ml.

Significant difference (P<0.05): *_vs_. that in the absence of Ca^{2+} ions.

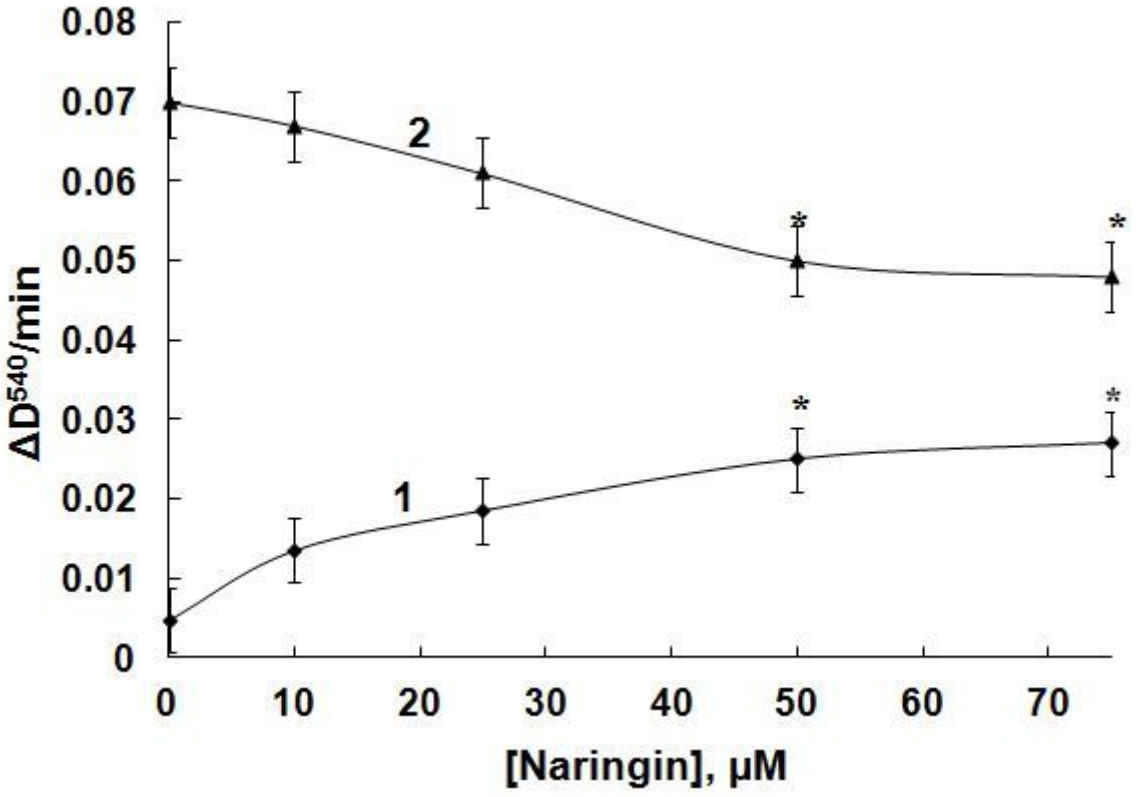

Figure 6

Effect of naringin on the rate of MPTP (ΔD^{540}/min) formation for rat heart mitochondria in the absence (1) and in the presence of free Ca^{2+} 550 mM (2).

0.12 M KCl, 0.005 M HEPES, 0.005 M KH_2PO_4, 0.002 M $MgCl_2$, and 0.00005 M EGTA, pH 7.4 at 26 ºC, 5 mM succinate as a substrate, 0.5 mg protein/ml.

Significant difference (P<0.05): *_vs_. that in the absence of naringin.

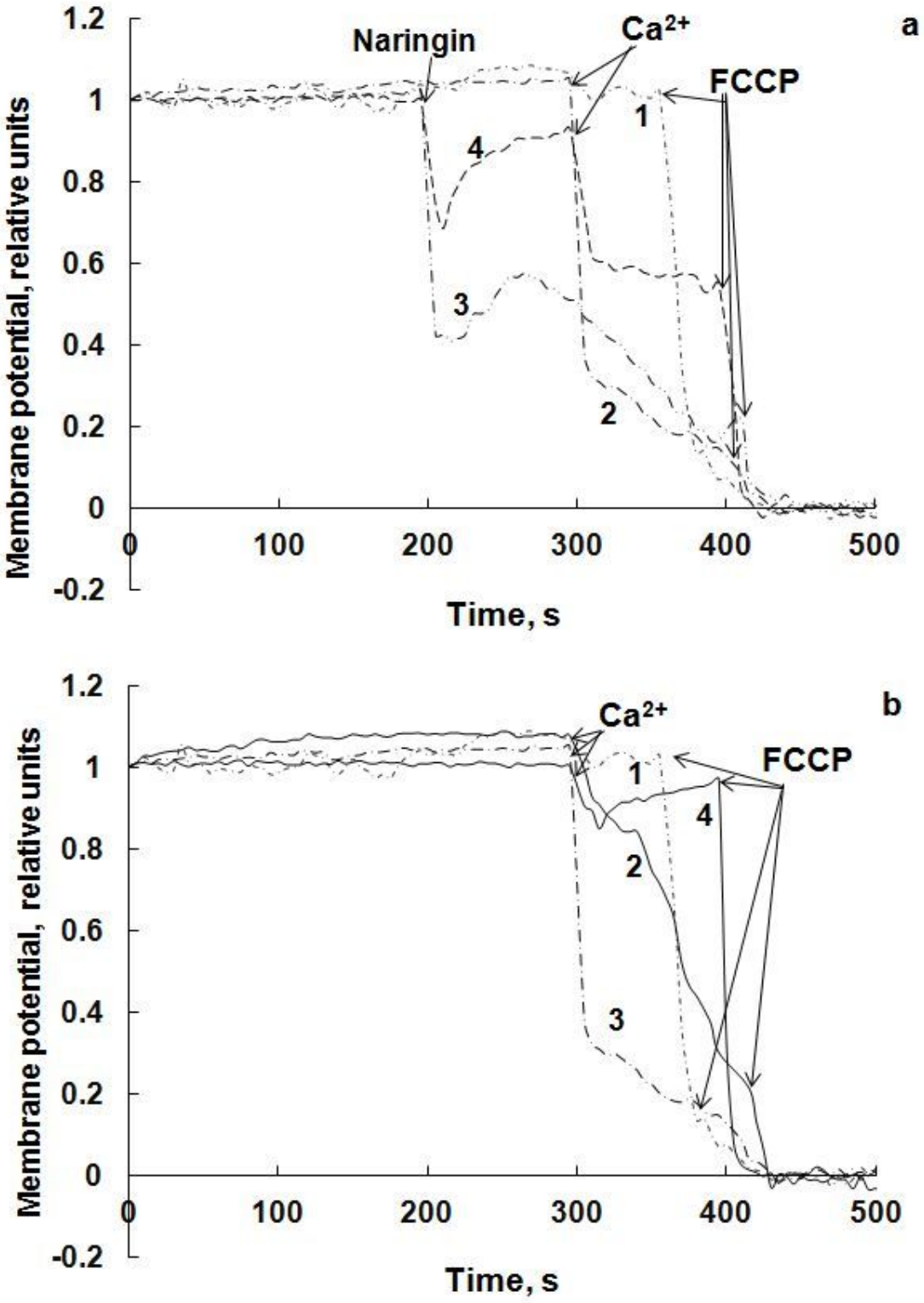

Figure 7

Representative traces of rat heart mitochondrial membrane potential dissipation: a) control (1); 550 μM Ca^{2+} (2); 75 μM naringin (3); 550 μM Ca^{2+} + 75 μM naringin + 10 μM RuR (4);

b) control (1); 100 μM Ca^{2+} (2); 550 μM Ca^{2+} (3); 550 μM Ca^{2+} + 10 μM RuR (4). Mitochondrial membrane potential was detected using the fluorescent dye safranin O (8 μM) at λex/λem 495/586 nm at 27 °C and

5 mM succinate as energizing substrate. Mitochondria (0.3 mg of protein/ml) were added to the medium at constant gentle stirring: 0.25 M sucrose, 0.005 M HEPES, 0.005 M KH_2PO_4, 0.002 M $MgCl_2$, 0.00005 M EGTA, and 5 mM succinate as a substrate, pH 7.4, at 26 °C.

Supplementary Files

This is a list of supplementary files associated with this preprint. Click to download.

- Abstract.jpg